RESEARCH PAPER

Microneedle-Mediated Delivery of Copper Peptide Through Skin

Hairui Li • Yong Sheng Jason Low • Hui Ping Chong • Melvin T. Zin • Chi-Ying Lee • Bo Li • Melvina Leolukman • Lifeng Kang

ABSTRACT

Purpose Copper peptide (GHK-Cu) plays an important role in skin regeneration and wound healing. However, its skin absorption remains challenging due to its hydrophilicity. Here we use polymeric microneedle array to pre-treat skin to enhance GHK-Cu skin penetration.

Methods Two *in vitro* skin models were used to assess the capability of microneedles in facilitating skin delivery of GHK-Cu. Histological assay and confocal laser scanning microscopy were performed to characterize and quantify the microconduits created by the microneedles inside skin. Cellular and porcine models were used to evaluate the safety of microneedle-assisted copper peptide delivery.

Results The depth and percentage of microneedle penetration were correlated with application forces, which in turn influenced the extent of enhancement in the skin permeability of GHK-Cu. In 9 h, 134 ± 12 nanomoles of peptide and 705 ± 84 nanomoles of copper permeated though the microneedle treated human skin, while almost no peptide or copper permeated through intact human skin. No obvious signs of skin irritation were observed with the use of GHK-Cu after microneedle pretreatment.

Conclusions It is effective and safe to enhance the skin permeation of GHK-Cu by using microneedles. This approach may be useful to deliver similar peptides or minerals through skin.

H. Li • Y. S. J. Low • H. P. Chong • L. Kang (✉)
Department of Pharmacy, National University of Singapore, 18 Science Drive 4, Singapore, Singapore 117543
e-mail: lkang@nus.edu.sg

H. Li • M. T. Zin • C.-Y. Lee • B. Li • M. Leolukman
3M Innovation Singapore, 100 Woodlands Avenue,
Singapore, Singapore 738205

ABBREVIATIONS

AAS	Atomic absorption spectroscopy
DMEM	Dulbecco's modified Eagle's medium
DMSO	Dimethyl sulfoxide
GHK	Glycyl-L-histidyl-L-lysyl
GHK-Cu	Copper peptide
HaCaT	Human adult low calcium high temperature
HDF	Human dermal fibroblasts
HPLC	High performance liquid chromatography
MN	Microneedle
MSS	Microchannel Skin System
MTT	3-(4,5-dimethylthiazol-2-yl)-2,5-diphenyl tetrazolium bromide
PBS	Phosphate buffered saline

INTRODUCTION

Glycyl-L-histidyl-L-lysyl (GHK) is a naturally occurring carrier tripeptide with high affinity for copper ions. GHK was first isolated from human plasma by Dr L. Pickart because of its activity to prolong survival of normal liver cells (1). Subsequently, researchers found that GHK-Cu can stimulate the synthesis of extracellular matrix macromolecules, such as collagen and glycosaminoglycan (2–4). It can activate the production of metalloproteinases and anti-proteases that remove damaged proteins from the extracellular matrix macromolecules (5). GHK-Cu was also found to increase decrorin expression and decrease TGF-beta expression, which is beneficial for a scar-free healing (6,7). The increased expression of p63 of keratinocytes by both GHK-Cu and GHK suggests that GHK and its copper complex can promote the survival of basal stem cells in skin (8,9). These contribute to the wound-

healing and skin remodelling effects of GHK-Cu (2,10–14). The biochemical action of GHK and GHK-Cu on skin cells were summarized in SI 1. Recent genomic studies revealed that GHK can directly modulate the expression of a large number of human genes and reverse gene expression to a healthier state, which may explain the diversity of its biological actions (15–17). Furthermore, *in vivo* studies showed that GHK-Cu can improve hair growth, skin regeneration and wound healing (10).

Minerals are essential for human health and mineral supplementation is recommended to complement dietary intake. Supplementation of minerals via oral route is the most common way. However, oral mineral absorption is affected by many factors including interactions with other dietary components in the gastrointestinal tract (18). Gastrointestinal side effects have also been reported with oral ingestion of some minerals, such as copper and iron. In addition, oral liquid forms of iron supplementation may cause teeth stains (19). To this end, transdermal delivery of minerals may be a useful alternative but remains largely unexplored. Copper as an essential trace element plays a critical role in diverse biological processes, such as haemoglobin synthesis and the stimulation of skin biomarkers including collagen and elastin (20). Copper also has an important role in the activation of key enzymes specific to tissue repair and in the cross-linking and maturation of collagen in healing wounds (19). Because of the gastrointestinal irritation that oral intake of copper can cause, transdermal delivery of copper can act as a good alternative, although skin absorption of charged ions is very low (21,22). It was found that when GHK is coupled with copper, the peptide silences the redox activity of copper, hence permitting the delivery of copper in a non-toxic form that can be subsequently utilized by the cells (8,23).

Although its biological actions start at picomole level, far higher dosages have been used in clinical trials, since the GHK-Cu uptake levels are very low through skin. On the other hand, if GHK-Cu is injected intradermally, GHK is rapidly cleared (95% clearance in 1 min). The fragility and rapid breakdown of GHK is the major obstacle for clinical and cosmetic applications (24). In clinical trials involving GHK-Cu, large variations were observed and its efficacy towards the healing of indolent human wounds or skin ulcers were not found (10,25,26). To address the concerns, a variety of chemical modification to GHK has been carried out to produce breakdown-resistant copper complexes, but none were found better than GHK-Cu (10).

The low uptake of GHK-Cu by skin is a common problem, similar to many other peptides and molecules. This is as the skin naturally functions to protect the human body from the external environment. So the molecules that can be delivered though skin are limited. As a general rule, only hydrophobic molecules with a molecular weight less than 500 Da are able to passively diffuse through the skin (27). GHK-Cu with a log P of −4.5 can represent hydrophilic peptides that have difficulty in penetrating into skin (11). Because of the diverse biological effects of GHK-Cu, along with its potential as a source of copper supplementation, it is of interest to find out a method to enhance its skin absorption.

To this end, we propose the use of microneedles, a minimally invasive but effective skin permeation enhancement method, to facilitate the effective and sustained delivery of GHK-Cu through skin. If an effective skin uptake of GHK-Cu is possible in a sustained manner with microneedle pretreatment, GHK-Cu is expected to better fulfil its biological effects.

Microneedles with lengths in the micron ranges can enhance skin permeability with no pain by breaching the *stratum corneum* layer of skin with self-administration (28). It has been shown that microneedles are associated with a lower risk of microbial infection than hypodermal needles (29). There are different methods of drug delivery to skin with microneedles, and microneedle pretreatment followed by a topical formulation has the advantage of possible extended release (30). Studies have shown that pretreatment of skin with microneedles can enhance delivery of topically applied formulations (31,32), including peptides (33).

In this study, we investigate the effectiveness of a commercial microneedle product, i.e., 3M™ Microchannel Skin System (MSS), in enhancing the skin permeability of copper peptide, using both rat and human skin models. Since MSS is hand-applied by using an applicator, the effect of different application forces was studied. In addition, we also carried out cell and animal testing to verify its safety.

MATERIALS AND METHODS

Materials

The 3M™ Microchannel Skin System (MSS) is illustrated in Fig. 1a. The plastic microneedle patch comprises of a rectangular grid of needles (13 by 27 array, or 351 needles) centred on an oval array. The microneedles have square pyramidal shape with a needle height of about 700 µm and a tip-to-tip needle spacing of 500 µm. GHK-Cu and GHK were purchased from McBiotec, Nanjing, China. The ratio of GHK to Cu is 2:1 (manufacturer data). Copper standard solution (1 g/L), and trypan blue solution (0.4%) were purchased from Sigma-Aldrich, Singapore. Concentrated nitric acid (69% *w/w*) was purchased from VWR International S.A.S, Singapore. Rhodamine B was purchased from Alfa Aesar (Lancaster, UK). Phosphate buffered saline (PBS) (pH 7.4, 10×) was obtained from Vivantis, Malaysia. PDMS (Sylgard® 184 Silicone Elastomer Kit) was purchased from Dow Corning (Midlan, MI, USA). Solvable™, an aqueous based tissue solubilizer, was purchased from PerkinElmer

Fig. 1 Depth of microneelde penetration measurement. (**a**) 3M™ MSS microneedle array and the individual needles. (**b**) Illustration of microneedle application with an applicator. (**c**) Indirect measurement of depth of penetration using rhodamine B-coated micrroneedles. The *yellow line* shows the depth of penetration. (**d**) Confocal image showing the fluorescent pattern of a single microchannel after microneedle application. (**e**) Histological section of rat skin stained with hematoxylin and eosin after microneedle application. The *yellow arrow* shows the breach of epidermis. (**f**) Depth of penetration against force of microneedle (MN) application.
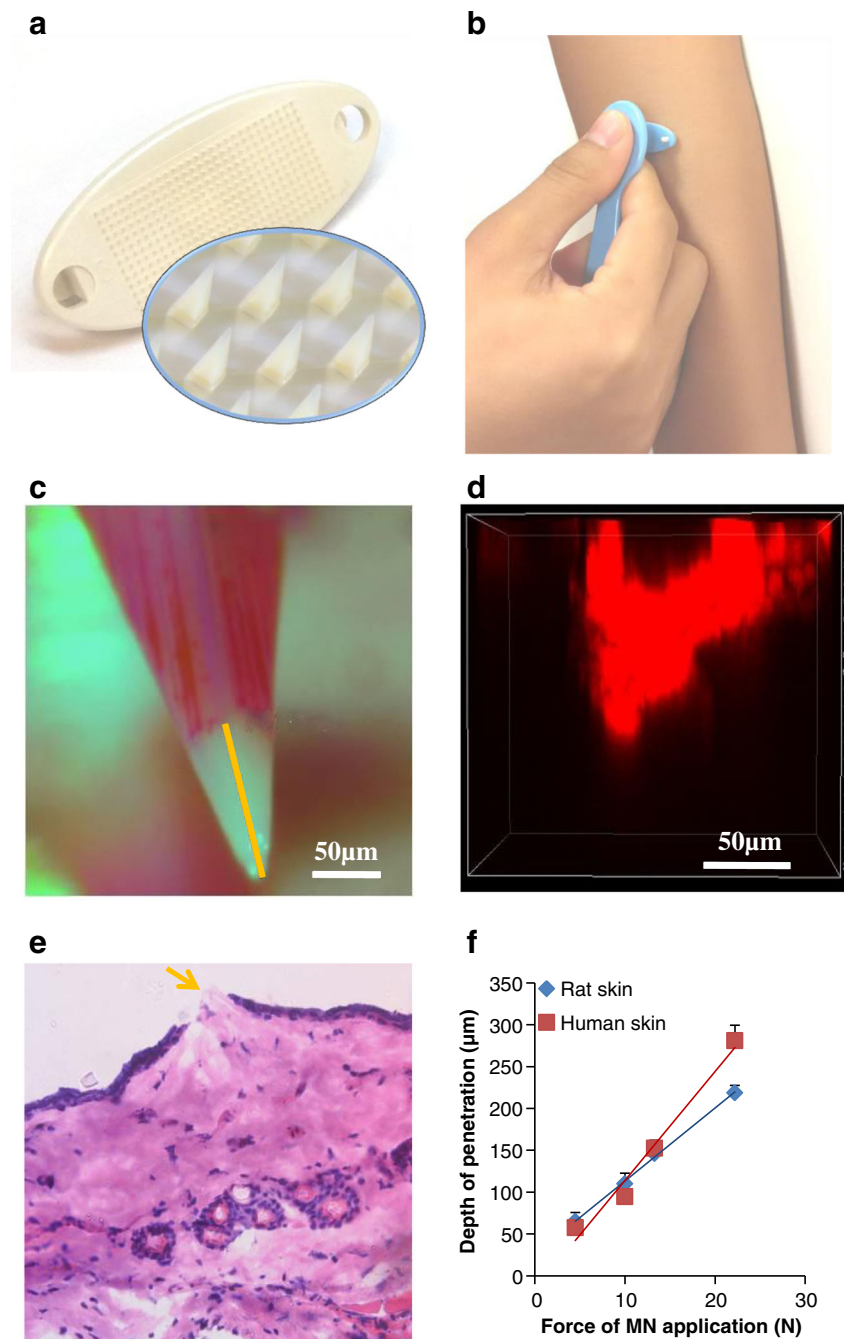
(Watham, MA, USA). Pierce® BCA protein assay kit was purchased from Thermo Scientific (Rockford, IL, USA). 3-(4,5-dimethylthiazol-2-yl)-2,5-diphenyl tetrazolium bromide (MTT) and dimethyl sulfoxide (DMSO) were purchased from MP Biomedicals, Singapore. Dulbecco's modified Eagle's medium (DMEM) and fetal bovine serum were purchased from Life Technology, Singapore. Penicillin streptomycin solution was purchased from PAN-Biotech GmbH, Germany. All chemicals were used as supplied.

Skin and Microneedle Application

Human dermatomed skin was obtained from Science Care (Phoenix, AZ, USA). The skin tissues were excised from the thighs of Caucasian female cadaver, who died at the age of 92.

Besides human skin, rat skin was also chosen for the *in vitro* skin permeation and penetration study. Skin of rodents, including rats, is the most commonly used for *in vitro* percunaeous permeation studies because of its availability (34). Rat abdominal skins were obtained from National

University of Singapore Comparative Medicine through the tissue sharing program. The hair on rat skin was removed by an electrical shaver followed by hair removal cream (Veet®) application and removal after 2 min. Subcutaneous fat and connective tissues were also trimmed off (35).

A 6 mm thick PDMS substrate was used to support the skin for microneedle application as reported (36). The skin was spread over the PDMS substrate mounted on a Styrofoam board with epidermis side up. A microneedle array was then put on the skin sample. Four different forces were applied through the applicator (Fig. 1b) at 4.5, 10.0, 13.3 and 22.2 N for 10 s, respectively, using a force gauge (HF-10, JISC, Japan).

The use of animal skin was approved by the National University of Singapore Institutional Animal Care and Use Committee. The use of human skin was approved by the National University of Singapore Institutional Review Board.

Depth of Microneedle Penetration Measurement

Microneedles were first primed with oxygen plasma in a plasma cleaner (Harrick Plasma, US) for 3 min to render them hydrophilic. The arrays were then flood-coated with 70 µl of 0.1% *w/w* rhodamine B solution and dried at 35°C for 1 h. The rhodamine B coated arrays were then applied with a force of 4.5, 10.0, 13.3 and 22.2 N for 10 s respectively on rat and human dermatomed skin samples. The depth of penetration was measured indirectly by recording the distance from the tip of the microneedles to the boundary where the rhodamine B coating was wiped off after skin insertion (31). To analyze the penetration depth of the microneedles, the microneedles were imaged using a stereoscopic microscope (Nikon SMZ25, Japan). The depth of penetration for each array was then determined by measuring 35 out of the total 351 microneedles per array. Three arrays were tested for each force.

Confocal laser scanning microscopy was used to visualize the micro-conduits created in rat skin placed on a piece of glass slide. The scanning started from the *stratum corneum* side, through the z-axis of the microscope (A1R+si, Nikon, Japan) at 10× magnification. The excitation wavelength was 562 nm and fluorescence emission was at 570–620 nm for rhodamine B.

Histological Examination

Histological examination of rat skin was carried out by cutting the microneedle treated skin samples into 10 µm sections using a Microcryostat (Leica, Germany). The histological sections were stained with hematoxylin and eosin and imaged using a microscope (Olympus, Japan).

Percentage of Penetration Measurement

The percentage of penetration was tested using trypan blue coated microneedles. Microneedle arrays were first treated with oxygen plasma for 3 min, flood-coated with 70 µl of trypan blue solution and then dried at 35°C for 1 h. After application of a microneedle array with the specified force on skin, the skin was cleansed with water. Application sites were then imaged by using the stereoscopic microscope. The visible insertions were counted and the percentage of penetration (the number of stained dots divided by the total number of array microneedles) was calculated. At least 3 replicates were performed at each force.

In Vitro Skin Permeation Study

Vertical Franz diffusion cells with an effective exposed area of 1 cm^2 were used. The pretreated skin samples were mounted onto Franz diffusion cells with epidermis facing up. The intact skin was used as control. The donor cell contained 2 ml of 5.8 mM (GHK)$_2$Cu (the molar ratio of GHK to Cu in the raw material was 2 to 1) solution while the receptor cell contained 4.8 ml of 1× PBS. The cells were placed inside a chamber with temperature controlled at 32°C (comparable to the physiological temperature of the skin surface). Magnetic stirrers in the receptor cells stirred at a speed of 100 rpm. The receptor solutions were withdrawn at pre-set time intervals and replaced with fresh ones. The receptor solutions were subjected to the measurement of copper permeated through the skin by atomic absorption spectroscopy (AAS) and the measurement of peptide permeated by high performance liquid chromatography (HPLC). At completion, the skin surface was washed by rinsing the donor and receptor compartments with 1 ml water 3 times, respectively. The skin was then removed from the diffusion cells, dried with Kimwipes and collected into Falcon tubes for the measurement of copper retained in skin by AAS (37). Three replicates were conducted for each group.

AAS Method

Copper concentrations were determined by using an atomic absorption spectrometer (PinAAcle 900T, PerkinElmer) with acetylene flow rate of 2.5 L/min and compressed air flow rate of 10 L/min. The instrument was calibrated with Cu working standards (1.57–62.95 µM) made from Cu stock standard solution (1 g/L) with 2% nitric acid as the diluent. Diluted permeation samples collected from receptor solutions were then aspirated into the air/acetylene flame where Cu atoms absorb light of 324.75 nm. All readings of standards and samples were conducted with the instrument in the absorbance mode. To digest skin tissues prior to analysis, concentrated nitric acid was used, as previous studies have shown that it quantitatively releases trace elements from biological tissues

(38). Nitric acid of 2.5 ml was added to each of the Falcon tubes containing skin samples and heated at 80°C using a thermostatic water bath until complete digestion of the skin samples (38). After that, they were topped up to 10 ml using deionized water and filtered using 0.22 μm polytetrafluoroethylene membrane. The filtered solution was used for the measurement of the amount copper retained in skin.

HPLC Method

The amount of GHK permeated was determined by using Hitachi L2000 LaChrome Elite HPLC system with Agilent Bio SCX NP3 column (50 mm×4.6 mm, 3 μm). The mobile phase consisted of Mobile A (Millipore water) and Mobile B (10 mM NaH_2PO_4 with 0.5 M NaCl) with a gradient elution program with a mixture of solvents A and B as follows: 0% B for 1 min, 1–100% B for 1–5 min, 100% B for 5–8 min, 100–0% B for 8–8.1 min, and 0% B for 8.1–11 min. The flow rate was set at 0.5 ml/min. The injection volume was 20 μl for each sampling and ultraviolet detection was performed at a wavelength of 218 nm. A calibration curve was conducted using GHK standard solution from 1.18 to 587.58 μM.

Skin Total Protein Determination

Skin samples were put into a 2 ml tube with 1.5 ml Solvable™ added. Then the tube was heated at 60°C for 4 h to allow the completely dissolution of skin. The total protein level of skin was determined by using a Pierce® BCA protein assay kit after the skin digestion solution was diluted appropriately with water.

Cytotoxicity Assay of GHK-Cu on Skin Cells

The cytotoxicity of different concentrations of GHK-Cu against human adult low calcium high temperature (HaCaT) keratinocytes and human dermal fibroblasts (HDF) were studied by MTT assay in 6 replicates. Briefly, 5000 cells in 200 μl culture medium (DMEM supplemented with 10% fetal bovine serum and 1% penicillin-streptomycin solution) per well were seeded into 96-well plates and incubated for 24 h. The culture medium was then removed. Subsequently, 180 μl fresh culture medium and 20 μl of GHK-Cu samples (0.058–58,000 μM $(GHK)_2Cu$ in PBS) were added per well and incubated for 24, 48 and 72 h, respectively. For control group, 180 μl fresh culture medium and 20 μl of PBS were added. At the respective analysis point, the medium was removed. The wells are washed with 200 μl PBS and replenished with 200 μl fresh medium per well. Twenty μl MTT solution (5 mg/ml in PBS) was added to each well, after which the plates were incubated for an additional 4 h. The supernatant was then removed and formazan crystals were solubilized in 150 μl DMSO. Absorbance was recorded at

595 nm with a microplate reader (Tecan, Switzerland). Wells containing DMSO alone were used as the blank. Percentage of cell viability was expressed as $(A_{sample}-A_{DMSO})/(A_{control}-A_{DMSO}) \times 100\%$.

In Vivo Irritation Test on Pigs

Young adult swine (Yorkshire X), ranging from 10 to 40 kg were used for the study. The animals were first sedated with ketamine (10 mg/kg) and then anesthetized with isoflurane gas. Atropine was administered to reduce salivary, tracheo-bronchial, and pharyngeal secretions. The ham area of pigs was shaved with an electrical shaver followed by a disposable shaver. The microneedles were applied on the skin with a hand force of around 20 N (estimated by using the force gauge) for 10 s. Then the skin was observed for irritation and imaged with time. In another testing, immediately after microneedle treatment, the application site was covered by gauze saturated with GHK-Cu solution, then fixed with plaster. After 8 h, the gauze was removed and the skin was imaged. The studies were repeated on 3 to 4 pigs. The pigs were later recovered. The procedure for animal testing was approved by the National University of Singapore Institutional Animal Care and Use Committee.

Statistical Analysis

All results were presented as mean±standard deviation. Statistical analysis was performed by one-way analysis of variance followed by Tukey *post hoc* test using IBM SPSS Statistics 19. A probability value of $p < 0.05$ was considered statistically significant.

RESULTS

Depth of Microneedle Penetration

In Fig. 1c, the yellow line indicated the distance from the tip of the microneedles to the boundary where the rhodamine B coating has been wiped off after skin insertion. The value of the distance was taken as depth of penetration of microneedles. Figure 1d showed the direct measurement of the depth of penetration using confocal laser scanning microscopy by measuring the depth of the microneedle fluorescence pattern inside the skin. The depth of penetration associated with an application force of 13.3 N on rat skin was measured to be 130 μm with direct measurement and 146 μm using indirect measurement. It was found that the results obtained from indirect depth of penetration measurement method had no difference from those obtained by direct measurement method ($p > 0.05$). Hence, the indirect method was used

for this study for its convenience. Furthermore, Fig. 1e further ascertained the presence of microscale passages created by microneedles inside the rat skin. Figure 1f showed that the depth of penetration of microneedles increased linearly with application force both on rat ($r^2 = 0.9977$) and human ($r^2 = 0.9758$) skin samples in the tested force range from 4.5 to 22.2 N.

Percentage of Penetration

The percentage of microneedle penetration in rat skin was measured using trypan blue coated microneedles. Figure 2a and b shows the representative image of rat skin, human dermatomed skin after application of trypan blue-coated microneedles at 22.2 N, respectively. The blue dots that remained on the skin indicated the successful penetration of microneedles into skin. The number of the blue dots was used to calculate the percentage of penetration per microneedle array. Figure 2c showed that a higher force of microneedle application resulted in a higher percentage of penetration.
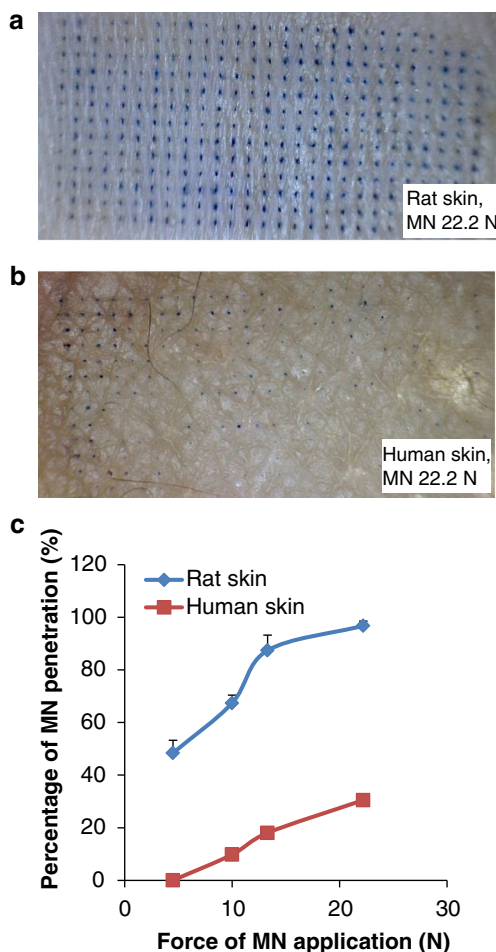

Fig. 2 Percentage of penetration. Representative images of 22.2 N MN application force on rat skin (**a**) and human dermatomed skin (**b**). (**c**) Percentage of penetration against force.

The increase in force of microneedle application on rat skin resulted in a sharper increase in the percentage of penetration as compared to that on human dermatomed skin. The highest force of 22.2 N made the percentage of penetration to be almost 100% on rat skin and 30% on human dermatomed skin.

In Vitro Skin Permeation Study

To assess the enhancing effects of the microneedles for GHK-Cu to permeate through skin at different forces of application, we performed *in vitro* drug permeation study. Upon topical administration, the copper ions are subjected to dynamic ligand exchange inside skin (37). Therefore, quantitative assessment of skin penetration of GHK-Cu is challenging. Hence, we analysed the permeation of copper and GHK separately by using AAS and HPLC. Figure 3a and b showed that the amounts of copper and peptide permeated through rat skin were significantly increased after microneedle pretreatment. Figure 3c and d showed that for non-treated human dermatomed skin, there was no peptide detected in the receptor solution, while only trace amount of copper was detected, which may be from the skin itself (data not shown). With the microneedle pretreatment, copper and peptide were detected in the receptor solution. However, substantial high amounts of copper and peptide were detected only when a high force (22.2 N) was used.

Figure 4 showed that there was no significant difference in the amount of copper retained in skin samples after 9 h' permeation study among the microneedle pretreated skin samples and the control at various forces. However, significant difference was found between rat and human skin.

Cytotoxicity Assay of GHK-Cu on Cells

Figure 5 showed that $(GHK)_2Cu$ was not toxic to either HaCaT keratinocytes or HDF cells in the range of 0.0058–5800 µM. Besides, GHK-Cu at 5800 µM showed certain stimulatory effect on HDF proliferation. Other research groups have also shown that GHK-Cu can stimulate the growth of dermal fibroblasts (39,40).

In Vivo Irritation Test on Pig Skin

For blank microneedles, minimal erythema was observed immediately after removal of microneedles. Mild erythema was observed at 5 min but almost not visible after 25 min (Fig. 6a). For GHK-Cu application immediately after microneedle pretreatment, no erythema or edema was observed for 8 h (Fig. 6b).

Fig. 3 *In vitro* skin permeation study. The cumulative amount of copper (**a**) and peptide (**b**) permeated through rat skin pretreated with varying application forces. The cumulative amounts of copper (**c**) and peptide (**d**) permeated through human dermatomed skin pretreated with varying application forces.
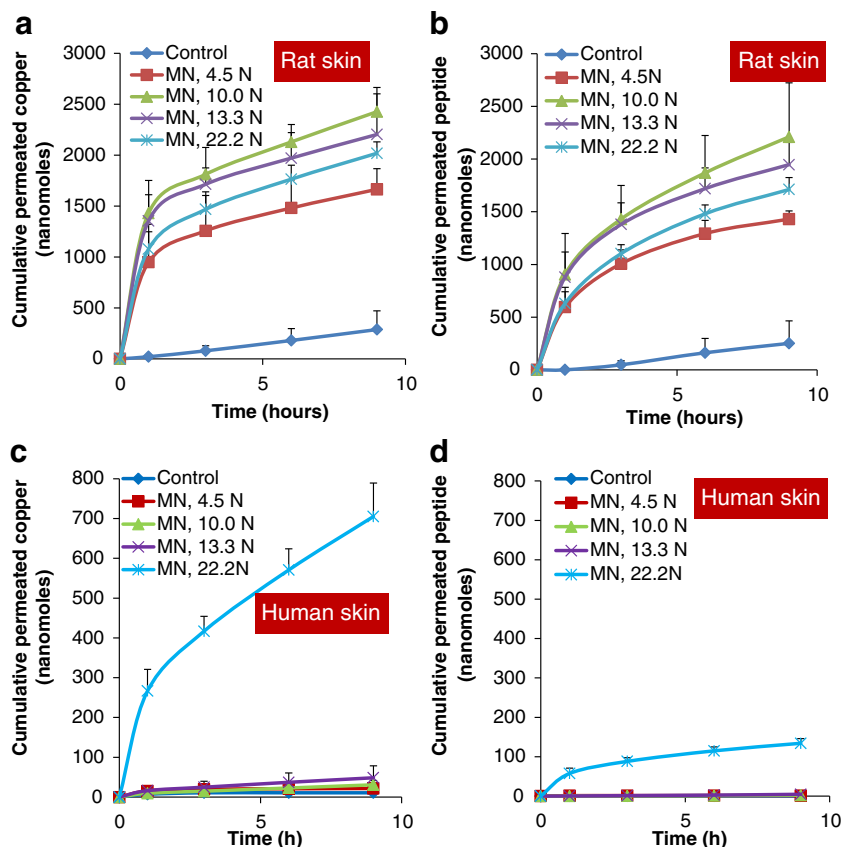
DISCUSSION

Microneedles can painlessly enhance the skin permeation of a wide range of therapeutic compounds which barely penetrate human skin (30). It has been reported that the microneedle application force can influence its enhancing effect (41–44). In this study we evaluated the skin permeation of topical GHK-Cu *in vitro* using a microneedle array from 3M Company. The 3M™ MSS is designed for manual application with a plastic applicator. The application forces tested were: 4.5 N (low), 10 N (medium), 13.3 N (medium) and 22.2 N (high).

To study the depth of needle penetration, two approaches have been used. One is the direct measurement of the microchannels inside skin by confocal laser scanning microscopy and the other is the indirect measurement. In the indirect measurement, the depth of penetration was obtained by measuring the length of needle tip where rhodamine B dye was wiped off (31). But the coating procedure of rhodamine B onto the microneedles was complicated. To simplify the microneedle coating procedure, we treated the microneedles with oxygen plasma, which was found to be very effective for rhodamine B coating.

Fig. 4 Cumulative amount of copper retained in skin after 9 h permeation study. The 'Clean skin' refers to the skin that was not used in permeation study.
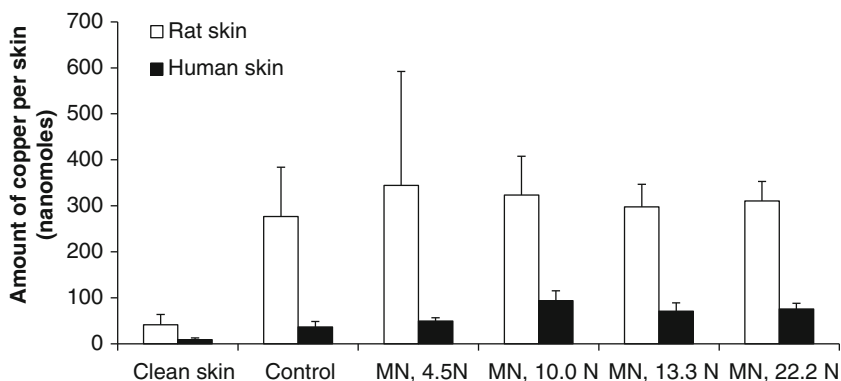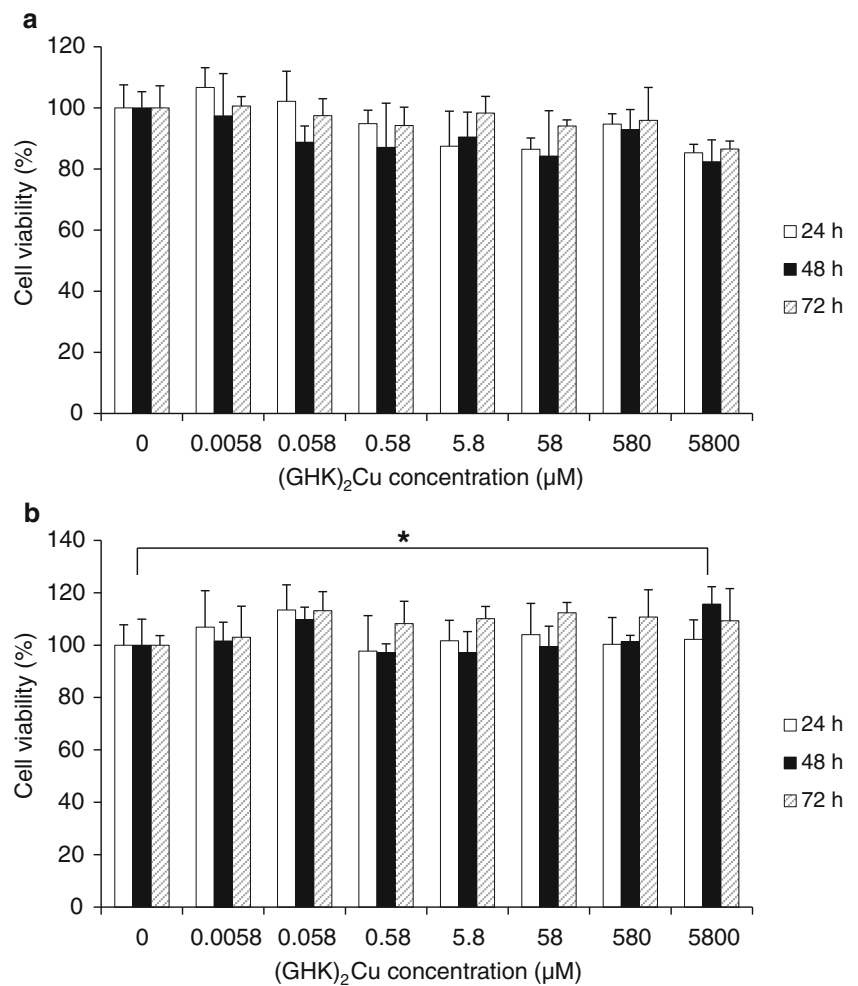
Fig. 5 Cytotoxicity study. Viability of HaCaT keratinocytes (**a**) and HDF (**b**) after incubation with GHK-Cu for 24, 48 and 72 h.

The linear relationship between depth of penetration and microneedle application force indicates that these two factors are strongly correlated. However, we cannot assume that the linearity will be the same when the force is out of the range (<4.5 N or >22.2 N) (45). The force range would be from 13 to 63 mN/needle in our study if converted to force per needle. Some of these forces are even lower than the insertion forces of reported microneedles. For example, Park *et al.* reports measured microneedle insertion force of 37 mN with a tip 20 µm in diameter (46). It indicated that our microneedle array had a high efficiency for skin insertion.

To study the percentage of penetration, trypan blue coated microneedles were used. Trypan blue is known to specifically stain the sites of *stratum corneum* perforation (47). A common procedure is to treat the skin first with microneedles, and then transfer trypan blue solution on the treated area for targeted

Fig. 6 Representative images of *in vivo* irritation test on pig skin. (**a**) The skin conditions after MN application. (**b**) The condition of MN pre-treated skin, followed by application of 5.8 mM copper peptide for 8 h. The marked rectangle area indicated the microneedle treated area.
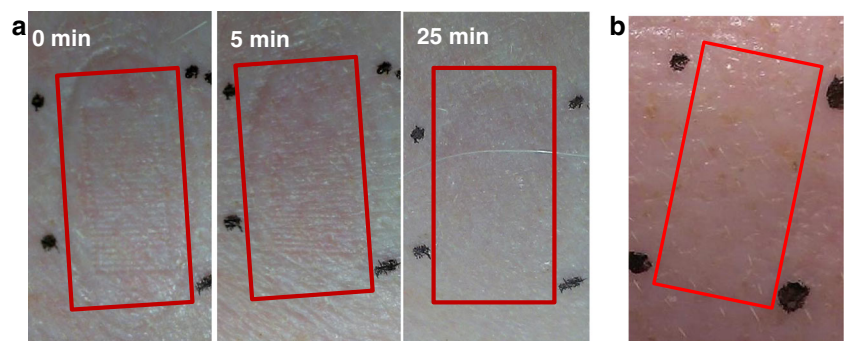
staining (42,47). However, we found that wrinkles and hair follicles can also be easily stained. Besides, trypan blue solution has limited contact with skin surfaces to ensure staining of all the microchannels because of the hydrophobic nature of skin surfaces. To solve this problem, we coated trypan blue directly onto the microneedles and then conducted the penetration test on skin. The false staining on the skin surface was then wiped off with water. With the new method, we can easily get clear staining images indicating the successful penetration of microneedles.

The results showed that with a higher force, the percentage of penetration increased. However, the effects were different on rat and human skins. Rat skin was much easier to be stained than human dermatomed skin. Trypan blue stains damaged cells selectively because the damaged cell membranes allow trypan blue to enter and stain the nuclei and cytoplasm (48). Since the *stratum corneum* is made up of layers of highly keratinized cells it will not be stained by trypan blue. Trypan blue can stain the epidermis at the sites of *stratum corneum* perforation (36). Although rat full skin and human dermatomed skin samples had the similar thickness, around 500 μm, rat skin has a much thinner layer of epidermis (~15 μm, Fig. 1e) than human skin (~200 μm). After the *stratum corneum* of rat skin is penetrated by microneedles, the viable epidermis below may be easily stained. On the other hand, the human skin has a more complicated structure. The layer below the *stratum corneum* is the *stratum granulosum*. Since the *stratum granulosum* is made up of partially keratinized cells without nuclei, it is more difficult to stain (49).

In general, microneedle pretreatment can increase skin delivery of GHK-Cu, although the results were quite different on rat and human skin. The permeation of copper peptide was observed for non-treated rat skin, but almost none for intact human dermatomed skin. With microneedle pretreatment, the permeated amount of copper and peptide increased significantly than those through non-treated rat skin (Fig. 3a and b). For human skin, microneedle pretreatment made permeated copper and peptide detectable. But substantial increase in the skin permeation was only observed at 22.2 N (Fig. 3c and d).

We noticed that the depth of penetration was proportional to application forces in both rat skin and human dermatomed skin models. For the rat skin, however, the microneedles can easily penetrate the entire epidermis at all the forces, as the thickness of epidermis of rat skin is ~15 μm (Fig. 1e). Epidermis, especially, its outermost layer, i.e., the *stratum corneum*, is the main barrier. Thus, the permeation of copper peptide through rat skin was independent of depth of penetration in rat skin model, similar to another finding (36). Bachhav *et al.* also found that the transport of lidocaine was independent of the depth of the microchannels created by laser after removal of *stratum corneum* (50).

In case of human dermatomed skin model, when microneedle application forces were no higher than 13.3 N, increase in skin permeation was observed because the *stratum corneum* was penetrated, while the distinct increase in the skin permeation at 22.2 N may be due to the penetration of whole epidermis layer (the epidermis layer of the human skin is ~200 μm). It indicated that viable epidermis layers are also significant permeation barriers (51).

Apart from the two types of skin models (rat full skin and human dermatomed skin), we also tested human epidermis. Human epidermis has been widely used in *in vitro* skin permeation experiment to study the conventional transdermal drug delivery (52). Human epidermis has also been used to study microneedle assisted transdermal drug delivery (44,53). However, in our study, it was shown that human epidermis, without the dermis layer, showed a much higher percentage of penetration with microneedles as compared to human dermatomed skin (SI 2 and SI 3). It may be because the thick dermis in the dermatomed skin could provide cushion effect and have absorbed some of the force applied onto the epidermal layer. Furthermore, a sharp increase in skin permeation of copper peptide was observed even with a mild microneedle application force on human epidermis (SI 3). As such rat skin and human epidermis may have their limitations as models to study the physical enhancement of skin by using microneedles (SI 4).

Furthermore, higher skin permeation of GHK-Cu can be obtained with the use of a higher concentration of GHK-Cu solution with microneedle treatment. However, no permeation of GHK-Cu was observed through intact human dermatomed skin even when the GHK-Cu concentration increased (SI 5). It suggested that increasing GHK-Cu concentration alone in topical formulations might not be a good choice to improve the effect of the GHK-Cu creams/gels.

The ratio of copper to peptide permeated though rat skin was around 1:1, while when human skin models were used, the ratio was much higher. It may be partly due to the fact that more copper were retained in rat skin than in human skin. Moreover, GHK-Cu complex can permeate at a faster rate than GHK alone (SI 6), which suggested a potentially useful approach to deliver minerals through skin.

Although it was found that application force was correlated with copper permeation through skin, no correlation was found between application force and copper retention inside skin. Partitioning of copper can be influenced by complexation with proteins in the skin (54). In this case, the skin proteins were probably saturated with copper at the end of the permeation study, thus no difference of copper was found inside the skin samples. On the other hand, the difference between rat skin and human dermatomed skin may be due to the difference of protein content in the two types of skin. The weight of skin was around 0.40 and 0.10 g while the protein content was around 36 and 10 mg for one piece of rat skin and human

dermatomed skin used in permeation study, respectively. The retained peptide in skin was not studied in this *in vitro* model since GHK peptide would degrade rapidly because of the existence of enzymes *in vivo* (55).

Besides the efficacy, the skin irritancy potential of this approach was also tested, using MTT assay to monitor the metabolic activity of keratinocytes and fibroblasts (56). The cytotoxicity assay showed that GHK-Cu was not toxic to HaCaT keratinocytes and human dermal fibroblasts in the range of 0.0058–5800 μM (Fig. 5). From the *in vitro* permeation study, the highest amount of copper retained in skin was around 600 nanomoles (Fig. 5). The weight of skin was ~0.4 g. So the retained copper can reach a concentration of ~150 μM by calculation, which is less than 5800 μM. Thus it is not expected to cause any skin irritations. Furthermore, irritation test on pig skin confirmed that the skin recovered quickly after microneedle application and the combination of microneedles and topical GHK-Cu formulation did not cause any skin irritation. The skin of the domestic pig is widely accepted as a suitable model for human skin for dermatological research and for percutaneous permeation studies because pig skin is usually considered as the closest in structure to human skin among different animal species (57). Pigs have also been used in the studies of microneedle assisted topical drug delivery (31,58). Nevertheless, it is still necessary to further confirm the safety of microneedle assisted GHK-Cu application on human subjects.

The recommended intake of copper for healthy adults is 0.9 and 1.3 mg/day by American Food and Nutrition Board and World Health Organization, respectively (59,60). In our study, about 705 nanomoles/cm^2 of copper can permeate through human skin with the assistance of microneedles in 9 h. And a steady flux of 48. 1 nanomoles/h/cm^2 was calculated from the permeation curve (Fig. 3c). Hence about 721 nanomoles/cm^2 of copper was expected to permeate through the skin in the next 15 h. Altogether there would be about 1426 nanomoles/cm^2 (which is about 0.091 mg/ cm^2) of copper permeating through human skin in 24 h with the assistance of microneedles. As a result, a patch size of 9 to 15 cm^2 may be designed to meet the daily intake requirement of copper.

CONCLUSION

The application force was found to affect the percutaneous delivery of copper peptide by influencing the depth and percentage of microneedle penetration through skin. The skin permeation of copper peptide can be enhanced by microneedle pretreatment at a high application force with minimal skin disturbance. In 9 h, 134±12 nanomoles of peptide and 705±84 nanomoles of copper can permeate though the pretreated human skin. It indicates that microneedles may be useful to deliver similar peptides or minerals through skin.

Besides, human epidermis and rat skin may not be suitable models for *in vitro* skin permeation study when microneedles are used.

REFERENCES

1. Pickart L, Thaler MM. Tripeptide in human serum which prolongs survival of normal liver cells and stimulates growth in neoplastic liver. Nat New Biol. 1973;243(124):85–7.
2. Maquart FX, Pickart L, Laurent M, Gillery P, Monboisse JC, Borel JP. Stimulation of collagen synthesis in fibroblast cultures by the tripeptide-copper complex glycyl-L-histidyl-L-lysine-Cu2+. FEBS Lett. 1988;238(2):343–6.
3. Buffoni F, Pino R, Dal Pozzo A. Effect of tripeptide-copper complexes on the process of skin wound healing and on cultured fibroblasts. Arch Int Pharmacodyn Ther. 1995;330(3):345–60.
4. Wegrowski Y, Maquart FX, Borel JP. Stimulation of sulfated glycosaminoglycan synthesis by the tripeptide-copper complex glycyl-L-histidyl-L-lysine-Cu2+. Life Sci. 1992;51(13):1049–56.
5. Siméon A, Emonard H, Hornebeck W, Maquart F-X. The tripeptide-copper complex glycyl-L-histidyl-L- lysine-Cu2+ stimulates matrix metalloproteinase-2 expression by fibroblast cultures. Life Sci. 2000;67(18):2257–65.
6. Siméon A, Wegrowski Y, Bontemps Y, Maquart FX. Expression of glycosaminoglycans and small proteoglycans in wounds: modulation by the tripeptide-copper complex glycyl-L-histidyl-L-lysine-Cu(2+). J Investig Dermatol. 2000;115(6):962–8.
7. McCormack MC, Nowak KC, Koch RJ. The effect of copper tripeptide and tretinoin on growth factor production in a serum-free fibroblast model. Arch Facial Plast Surg. 2001;3(1):28–32.
8. Kang YA, Choi HR, Na JI, Huh CH, Kim MJ, Youn SW, *et al.* Copper-GHK increases integrin expression and p63 positivity by keratinocytes. Arch Dermatol Res. 2009;301(4):301–6.
9. Choi HR, Kang YA, Ryoo SJ, Shin JW, Na JI, Huh CH, *et al.* Stem cell recovering effect of copper-free GHK in skin. J Pept Sci. 2012;18(11):685–90.
10. Pickart L. The human tri-peptide GHK and tissue remodeling. J Biomater Sci Polym Ed. 2008;19(8):969–88.
11. Hostynek JJ, Dreher F, Maibach HI. Human skin retention and penetration of a copper tripeptide in vitro as function of skin layer towards anti-inflammatory therapy. Inflamm Res. 2010;59(11): 983–8.
12. Philips N, Hwang H, Chauhan S, Leonardi D, Gonzalez S. Stimulation of cell proliferation and expression of matrixmetalloproteinase-1 and interluekin-8 genes in dermal fibroblasts by copper. Connect Tissue Res. 2010;51(3):224–9.
13. Maquart FX, Bellon G, Chaqour B, Wegrowski J, Patt LM, Trachy RE, *et al.* In vivo stimulation of connective tissue accumulation by the tripeptide-copper complex glycyl-L-histidyl-L-lysine-Cu2+ in rat experimental wounds. J Clin Invest. 1993;92(5):2368–76.
14. Gorouhi F, Maibach HI. Role of topical peptides in preventing or treating aged skin. Int J Cosmet Sci. 2009;31(5):327–45.
15. Lamb J. The connectivity map: a new tool for biomedical research. Nat Rev Cancer. 2007;7(1):54–60.

16. Iorio F, Bosotti R, Scacheri E, Belcastro V, Mithbaokar P, Ferriero R, et al. Discovery of drug mode of action and drug repositioning from transcriptional responses. Proc Natl Acad Sci U S A. 2010;107(33):14621–6.

17. Campbell JD, McDonough JE, Zeskind JE, Hackett TL, Pechkovsky DV, Brandsma CA, et al. A gene expression signature of emphysema-related lung destruction and its reversal by the tripeptide GHK. Genome Med. 2012;4(8):67.

18. Harvey L. Mineral bioavailability. Nutr Food Sci. 2001;31(4):179–82.

19. Driscoll MS, Kwon EK, Skupsky H, Kwon SY, Grant-Kels JM. Nutrition and the deleterious side effects of nutritional supplements. Clin Dermatol. 2010;28(4):371–9.

20. Chan S, Gerson B, Subramaniam S. The role of copper, molybdenum, selenium, and zinc in nutrition and health. Clin Lab Med. 1998;18(4):673–85.

21. Araya M, Pena C, Pizarro F, Olivares M. Gastric response to acute copper exposure. Sci Total Environ. 2003;303(3):253–7.

22. Reynolds JEF, Prasad AB, editors. Martindale, the extra pharmacopoeia. 28th ed. London: The Pharmaceutical Press; 1982.

23. Pickart L, Freedman JH, Loker WJ, Peisach J, Perkins CM, Stenkamp RE, et al. Growth-modulating plasma tripeptide may function by facilitating copper uptake into cells. Nature. 1980;288(5792):715–7.

24. Pickart L. The need for improved skin regenerative copper peptides. Skinbiology.com. 2014. http://skinbiology.com/copper-peptides-need-for-improved.html. Accessed 17 Apr 2014.

25. Mulder GD, Patt LM, Sanders L, Rosenstock J, Altman MI, Hanley ME, et al. Enhanced healing of ulcers in patients with diabetes by topical treatment with glycyl-l-histidyl-l-lysine copper. Wound Repair Regen. 1994;2(4):259–69.

26. Bishop JB, Phillips LG, Mustoe TA, VanderZee AJ, Wiersema L, Roach DE, et al. A prospective randomized evaluator-blinded trial of two potential wound healing agents for the treatment of venous stasis ulcers. J Vasc Surg. 1992;16(2):251–7.

27. Prausnitz MR, Langer R. Transdermal drug delivery. Nat Biotechnol. 2008;26:1261–8.

28. Li H, Yu Y, Faraji Dana S, Li B, Lee CY, Kang L. Novel engineered systems for oral, mucosal and transdermal drug delivery. J Drug Target. 2013;21(7):611–29.

29. Donnelly R, Singh T, Tunney M, Morrow DJ, McCarron P, O'Mahony C, et al. Microneedle arrays allow lower microbial penetration than hypodermic needles in vitro. Pharm Res. 2009;26(11):2513–22.

30. Kim YC, Park JH, Prausnitz MR. Microneedles for drug and vaccine delivery. Adv Drug Deliv Rev. 2012;64(14):1547–68.

31. Duan D, Moeckly C, Gysbers J, Novak C, Prochnow G, Siebenaler K, et al. Enhanced delivery of topically-applied formulations following skin pre-treatment with a hand-applied, plastic microneedle array. Curr Drug Deliv. 2011;8:557–65.

32. Wu Y, Qiu Y, Zhang S, Qin G, Gao Y. Microneedle-based drug delivery: studies on delivery parameters and biocompatibility. Biomed Microdevices. 2008;10(5):601–10.

33. Mohammed YH, Yamada M, Lin LL, Grice JE, Roberts MS, Raphael AP, et al. Microneedle enhanced delivery of cosmeceutically relevant peptides in human skin. PLoS One. 2014;9(7):e101956.

34. Godin B, Touitou E. Transdermal skin delivery: predictions for humans from in vivo, ex vivo and animal models. Adv Drug Deliv Rev. 2007;59(11):1152–61.

35. Mah CS, Kochhar JS, Ong PS, Kang L. A miniaturized flow-through cell to evaluate skin permeation of endoxifen. Int J Pharm. 2013;441(1–2):433–40.

36. Kochhar JS, Quek TC, Soon WJ, Choi J, Zou S, Kang L. Effect of microneedle geometry and supporting substrate on microneedle array penetration into skin. J Pharm Sci. 2013;102(11):4100–8.

37. Hostynek JJ, Dreher F, Maibach HI. Human skin penetration of a copper tripeptide in vitro as a function of skin layer. Inflamm Res. 2011;60(1):79–86.

38. Tinggi U, Maher W. Determination of trace elements in biological tissues by aluminum block digestion and spike-height flame atomic absorption spectrometry. Microchem J. 1986;33(3):304–8.

39. Huang PJ, Huang YC, Su MF, Yang TY, Huang JR, Jiang CP. In vitro observations on the influence of copper peptide aids for the LED photoirradiation of fibroblast collagen synthesis. Photomed Laser Surg. 2007;25(3):183–90.

40. Pollard JD, Quan S, Kang T, Koch RJ. Effects of copper tripeptide on the growth and expression of growth factors by normal and irradiated fibroblasts. Arch Facial Plast Surg. 2005;7(1):27–31.

41. Oh JH, Park HH, Do KY, Han M, Hyun DH, Kim CG, et al. Influence of the delivery systems using a microneedle array on the permeation of a hydrophilic molecule, calcein. Eur J Pharm Biopharm. 2008;69(3):1040–5.

42. Verbaan FJ, Bal SM, van den Berg DJ, Dijksman JA, van Hecke M, Verpoorten H, et al. Improved piercing of microneedle arrays in dermatomed human skin by an impact insertion method. J Control Release. 2008;128(1):80–8.

43. Wu XM, Todo H, Sugibayashi K. Effects of pretreatment of needle puncture and sandpaper abrasion on the in vitro skin permeation of fluorescein isothiocyanate (FITC)-dextran. Int J Pharm. 2006;316(1–2):102–8.

44. Yan G, Warner KS, Zhang J, Sharma S, Gale BK. Evaluation needle length and density of microneedle arrays in the pretreatment of skin for transdermal drug delivery. Int J Pharm. 2010;391(1–2):7–12.

45. Davis SP, Landis BJ, Adams ZH, Allen MG, Prausnitz MR. Insertion of microneedles into skin: measurement and prediction of insertion force and needle fracture force. J Biomech. 2004;37(8):1155–63.

46. Park JH, Yoon YK, Choi SO, Prausnitz MR, Allen MG. Tapered conical polymer microneedles fabricated using an integrated lens technique for transdermal drug delivery. IEEE Trans Biomed Eng. 2007;54(5):903–13.

47. Kochhar JS, Goh WJ, Chan SY, Kang L. A simple method of microneedle array fabrication for transdermal drug delivery. Drug Dev Ind Pharm. 2012;39(2):299–309.

48. Tran S-L, Puhar A, Ngo-Camus M, Ramarao N. Trypan blue dye enters viable cells incubated with the pore-forming toxin HlyII of bacillus cereus. PLoS ONE. 2011;6(9):e22876.

49. Marieb EN, Hoehn K. Human anatomy & physiology. Boston: Pearson; 2007.

50. Bachhav YG, Summer S, Heinrich A, Bragagna T, Böhler C, Kalia YN. Effect of controlled laser microporation on drug transport kinetics into and across the skin. J Control Release. 2010;146:31–6.

51. Andrews SN, Jeong E, Prausnitz MR. Transdermal delivery of molecules is limited by full epidermis, not just stratum corneum. Pharm Res. 2013;30(4):1099–109.

52. Robert LB, Jeffrey JY, Margaret EKK. Determination of percutaneous absorption by in vitro techniques. Percutaneous Absorption: CRC Press; 2005. p. 265–9.

53. Park JH, Allen MG, Prausnitz MR. Biodegradable polymer microneedles: fabrication, mechanics and transdermal drug delivery. J Control Release. 2005;104(1):51–66.

54. Hostynek JJ. Factors determining percutaneous metal absorption. Food Chem Toxicol. 2003;41(3):327–45.

55. Endo T, Miyagi M, Ujiie A. Simultaneous determination of glycyl-L-histidyl-L-lysine and its metabolite, L-histidyl-L-lysine, in rat plasma by high-performance liquid chromatography with post-column derivatization. J Chromatogr B Biomed Sci Appl. 1997;692(1):37–42.

56. Gibbs S. In vitro irritation models and immune reactions. Skin Pharmacol Physiol. 2009;22(2):103–13.

57. Simon GA, Maibach HI. The pig as an experimental animal model of percutaneous permeation in man: qualitative and quantitative observations—an overview. Skin Pharmacol Appl Ski Physiol. 2000;13(5):229–34.

58. Zhang Y, Brown K, Siebenaler K, Determan A, Dohmeier D, Hansen K. Development of lidocaine-coated microneedle product for rapid, safe, and prolonged local analgesic action. Pharm Res. 2012;29:170–7.

59. Food and Nutrition Board, Institute of Medicine. Dietary reference intakes for vitamin A, vitamin K, arsenic, boron, chromium, copper, iodine, iron, manganese, molybdenum, nickel, silicon, vanadium, and zinc. 2015. http://www.nal.usda.gov/fnic/DRI/DRI_Vitamin_A/vitamin_a_full_report.pdf. Accessed 19 Jan 2015.

60. WHO/FAO/IAEA. Trace elements in human nutrition and health. 2015. http://whqlibdoc.who.int/publications/1996/9241561734_eng_fulltext.pdf. Accessed 19 Jan 2015.